

Trajectory Planning Using Reinforcement Learning for Interactive Overtaking Maneuvers in Autonomous Racing Scenarios

Levent Ögretmen, Mo Chen, Phillip Pitschi, and Boris Lohmann

Abstract—Conventional trajectory planning approaches for autonomous racing are based on the sequential execution of prediction of the opposing vehicles and subsequent trajectory planning for the ego vehicle. If the opposing vehicles do not react to the ego vehicle, they can be predicted accurately. However, if there is interaction between the vehicles, the prediction loses its validity. For high interaction, instead of a planning approach that reacts exclusively to the fixed prediction, a trajectory planning approach is required that incorporates the interaction with the opposing vehicles. This paper demonstrates the limitations of a widely used conventional sampling-based approach within a highly interactive blocking scenario. We show that high success rates are achieved for less aggressive blocking behavior but that the collision rate increases with more significant interaction. We further propose a novel Reinforcement Learning (RL)-based trajectory planning approach for racing that explicitly exploits the interaction with the opposing vehicle without requiring a prediction. In contrast to the conventional approach, the RL-based approach achieves high success rates even for aggressive blocking behavior. Furthermore, we propose a novel safety layer (SL) that intervenes when the trajectory generated by the RL-based approach is infeasible. In that event, the SL generates a sub-optimal but feasible trajectory, avoiding termination of the scenario due to a not found valid solution.

I. INTRODUCTION

Conventional trajectory planning for autonomous racing consists of a sequential execution of prediction and planning [1]. Initially, the movement of the opposing vehicles is predicted based on specific assumptions. Subsequently, the trajectory of the ego vehicle is planned, avoiding collisions with the assumed prediction. This sequential approach is suitable if the behavior of the opposing vehicles is independent of the ego vehicle. However, if an interaction exists between the vehicles, i.e., the opposing vehicles react to the behavior of the ego vehicle, no correct prediction can be determined.

An example of such an interactive scenario is an overtaking attempt, which the opposing vehicle actively tries to prevent by blocking. If the blocking vehicle is predicted to maintain a constant distance from a track boundary and the track is sufficiently wide, an overtaking maneuver is initiated. After starting to overtake, however, the blocking vehicle reacts immediately and thus deviates from the previous prediction. Overall, no valid prediction can be stated since the planning depends on the prediction, and in turn, the behavior of the opposing vehicle depends on the planned trajectory. This simple example encourages using more advanced interaction-aware planning approaches that avoid the

sequential execution of prediction and planning. A promising approach for this is RL, which allows for learning complex policies in high-dimensional environments with non-linear interaction and dynamics [2].

This paper examines the interactive scenario described above, in which a blocking vehicle is to be overtaken. In this scenario, we evaluate an existing, widely used conventional planning approach and demonstrate its limitations. Further, we propose a novel RL-based planning approach that explicitly exploits the interaction with the blocking vehicle and evaluate its performance and generalization ability. Additionally, we introduce an SL that counters infeasible trajectories caused by a lack of generalization of the RL-based approach.

A. Related Work

Conventional trajectory planning approaches require a prediction of the opposing vehicles, which is generated based on underlying assumptions. In current autonomous racing series, such as the Indy Autonomous Challenge (IAC)¹, with strict racing rules, often a constant speed and distance to the track boundary is assumed by the teams, as in [3]–[5]. For the subsequent trajectory planning, there are sampling-based, graph-based, and optimization-based approaches [1]. A commonly used sampling-based approach proposed in [6] for traffic scenarios is to generate a set of jerk-optimal trajectories by sampling the end state. The trajectories are checked for feasibility, and the optimal valid one is selected according to a pre-defined cost function. The described concept is applied similarly in [4], [5] for racing on oval tracks. The approach is extended in [7] to complex racing circuits with further consideration of the three-dimensional effects of the track. In [8], the jerk-optimal trajectories are used within a graph-based approach to connect the vehicle state with an offline computed spatio-temporal graph.

In addition to the conventional methods, there exist RL-based motion planning methods, which are summarized in [9]. In these methods, a general distinction is made between the action space, i.e., the level of control over the vehicle. On one side, there are low-level approaches in which the control inputs of the vehicle, e.g., acceleration and steering angle, are selected directly. On the other side, there are high-level approaches in which a maneuver, such as lane change left/right, keep lane, accelerate, or brake, is selected from a discrete finite set, and a fixed underlying movement is executed. The low-level approaches have been applied extensively for solo racing [10]–[13], which naturally does

All authors are with the Chair of Automatic Control, Department of Mechanical Engineering, TUM School of Engineering and Design, Technical University of Munich, 85748 Garching, Germany {levent.oegretmen, ge64mah, phillip.pitschi, lohmann}@tum.de

¹<https://indyautonomouschallenge.com>

not include interaction. A few studies have also examined overtaking in a multi-vehicle racing scenario [14]–[16]. In [14] and [15], the opposing vehicles follow either a fixed or random trajectory without interaction. In [16], the opponent vehicles are controlled by built-in game agents and older versions of the RL agent, with no information on their interaction. The direct control of the vehicle using these low-level methods provides the greatest possible freedom of maneuvers but can make training more complex, as the entire dynamics of the vehicle must be learned. In addition, an application on a real vehicle is safety-critical, as the directly applied inputs can lead to unsafe behavior due to modeling inaccuracies between the training model and the real vehicle. In contrast, the high-level approaches operate on a more abstract level, making them less safety-critical for real-world application. However, they are less suitable for the racing scenario since a restriction to a discrete, finite set of maneuvers does not adequately represent all necessary maneuvers in the mainly unconstrained racing scenario. Such approaches are often used in highway scenarios instead, as the definition of meaningful maneuvers is easier due to the structured environment with lanes.

Instead of the high- or low-level approaches mentioned above, it is also possible to plan a trajectory directly. Compared to the low-level approaches, trajectory generation is preferable from a safety point of view, as the mapping to control inputs is performed by a conventional controller that can be tuned to the specific vehicle being used. Compared to the high-level approaches, there is no need to define a set of discrete high-level maneuvers with fixed underlying trajectories, allowing for more diverse trajectories. Direct trajectory generation has been used for traffic scenarios, but to the authors’ knowledge, there is no application for racing. The trajectory is usually generated by utilizing an underlying structure to reduce the complexity of the training process. The authors of [17] utilize the same procedure as in [6] to generate a set of jerk-optimal trajectories by sampling the end state and use the weighting parameters of the cost function as the action space. While this approach is sufficient for traffic scenarios, it is less suitable for racing as it is limited to the generated set of trajectories, preventing the realization of more complex maneuvers. In [18], no sampling is performed, and instead, the end state of the jerk-optimal trajectory is used as the action space, which allows for more diverse maneuvers. If the end state chosen by the RL agent leads to an infeasible trajectory, the scenario is terminated immediately unsuccessfully.

For completeness, it should be mentioned that in addition to the RL-based approaches described here, game-theoretical approaches are also used for interactive planning. However, in contrast to RL-based approaches, they require increased online computing times, as a time-consuming game has to be solved in each execution step. In [19], a two-player blocking game is examined, and a bi-matrix game is solved based on sampled trajectory candidates. In [20], the trajectories of the individual vehicles are optimized iteratively, while the trajectories of the opposing vehicles are fixed.

B. Contribution

In contrast to existing literature, we focus in this work on interactive overtaking for autonomous racing and compare a conventional trajectory planning approach to a novel RL-based approach. The main contributions are summarized as follows:

- We introduce a highly interactive blocking scenario with a rule-based blocking agent, evaluate a commonly used conventional sampling-based trajectory planning approach in this setting, and show its limitations.
- We propose an RL-based trajectory planning approach for the introduced blocking scenario. In contrast to existing approaches for racing with a low-level action space, the trajectory is generated directly, avoiding the drawbacks described in Section I-A. The approach is evaluated in the blocking scenario and compared with the conventional approach.
- For the RL-based approach, we introduce an SL that intervenes if the generated trajectory is infeasible. In this case, a set of trajectories is generated, and the valid, most similar trajectory is selected. Thus, in contrast to existing approaches, infeasibility does not terminate the scenario, increasing the success rate.

The remainder of this paper is structured as follows: Section II contains introductory preliminary remarks on RL. The interactive blocking scenario considered here, including the behavior of the blocking vehicle, is presented in Section III. Section IV presents the conventional sampling-based and the proposed RL-based trajectory planning approach with the SL. The evaluation of both approaches in the blocking scenario is carried out in Section V, followed by a summary and an outlook for further research in Section VI.

II. REINFORCEMENT LEARNING PRELIMINARIES

RL is a method where an agent learns by interacting with an environment in a try-and-error style. A Markov Decision Process (MDP) mathematically formalizes the RL problem with the tuple $(\mathfrak{s}, \mathfrak{a}, P(s'|s, a), R(s, a), \gamma)$. \mathfrak{s} and \mathfrak{a} are the state space and action space, respectively. When being in state $s \in \mathfrak{s}$ and choosing action $a \in \mathfrak{a}$, the state transition function $P(s'|s, a)$ describes the probability of ending up in the state $s' \in \mathfrak{s}$. $R(s, a)$ is the expected reward the agent receives for this transition. The RL agent chooses the action a according to a policy $\pi(a|s)$. The goal of RL is to find a policy that maximizes the return $G_t = \sum_{k=t+1}^{T_{\text{ep}}} \gamma^{k-t-1} R_k$, which is the discounted sum of all future rewards from the current time step t to the terminal time step T_{ep} of the episode. The discount factor $\gamma \in [0, 1)$ scales how much the future rewards are worth compared to immediate rewards. The value function $v_\pi(s) = \mathbb{E}_\pi[G_t|s]$ for a given policy is defined as the expected return when being in state s and thereafter following the policy $\pi(a|s)$. [21]

RL algorithms reach their goal by learning the value function (value-based) or a policy directly (policy-based). Methods that use both are called actor-critic algorithms. The actor is the policy $\pi(a|s)$ that acts on the environment.

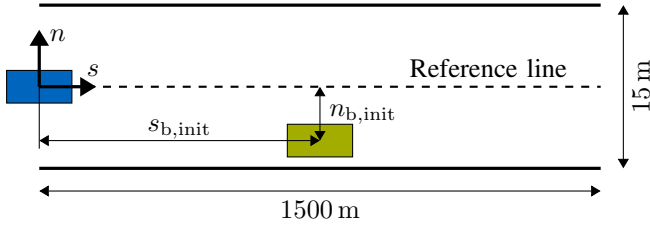


Fig. 1. Initialization of the blocking scenario with the overtaking vehicle (blue) at position $(s_{o,init} = 0 \text{ m}, n_{o,init} = 0 \text{ m})$ and the blocking vehicle (green) at $(s_{b,init}, n_{b,init})$. The reference line of the considered straight race track (not to scale) is depicted as a dashed black line.

The critic is the value function $v_\pi(s)$ that evaluates the reaction of the environment. One widely used representative of this method is the proximal policy optimization (PPO) algorithm [22]. It improves the general actor-critic approach by constraining the size of the policy updates.

RL algorithms are often combined with curriculum learning to improve the results. This method divides the learning procedure into multiple tasks with usually increasing complexity. The RL algorithm learns from the samples generated from one task and transfers the gained knowledge to the next task until it arrives at the final task. [23], [24]

III. BLOCKING SCENARIO

The blocking scenario under consideration is introduced with the used race track in Section III-A, the general scenario description in Section III-B, and the behavior of the blocking vehicle in Section III-C.

A. Race Track

The blocking scenario is carried out on a straight track without inclination or banking. The track is 1500 m long and 15 m wide. The center line of the track is used as the reference line with which the curvilinear coordinates s and n can be defined. While s corresponds to the progress along the reference line, n is the lateral offset along the corresponding normal vector. Although the orientation $\theta_r(s)$ and curvature $\kappa_r(s)$ of the reference line are 0 for straight tracks, they are accounted for in the following expressions for reasons of generality. Finally, we denote the distance between the reference line and the left and right track boundary with $n_l = 7.5 \text{ m}$ and $n_r = 7.5 \text{ m}$.

B. Scenario Description and Goal

A scenario consisting of two vehicles is considered on the introduced track, as illustrated in Fig. 1. The overtaking vehicle (variables denoted with index o) is initialized on the reference line at the beginning of the track with $s_{o,init} = 0 \text{ m}$ and $n_{o,init} = 0 \text{ m}$. The opposing blocking vehicle (variables denoted with index b) is initialized with a longitudinal gap at $s_{b,init} > 0$ and a lateral offset $n_{b,init}$. Both vehicles are initialized with the same velocity $v_{init} > 0$.

The blocking vehicle has a fixed rule-based blocking behavior described in Section III-C. For the overtaking vehicle, however, trajectories are planned using the conventional or RL-based approach, both introduced in Section IV, and it is

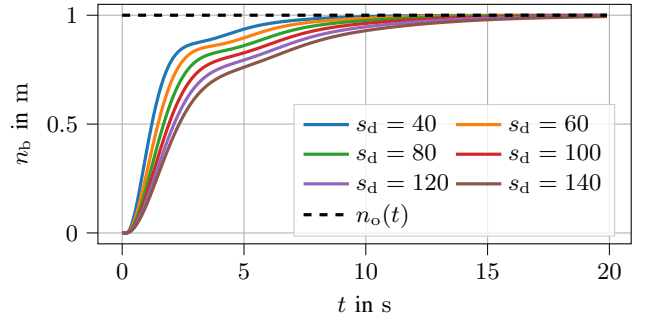


Fig. 2. Step responses for different values of s_d with $k_p = 0.05$, $k_d = 0.6$, and $k_n = 1.0$. The aggressiveness of the blocking maneuver increases with lower values of s_d .

assumed that the planned trajectories are followed exactly. The scenario ends successfully if the blocking vehicle is overtaken. However, if a planned trajectory is not feasible, a collision occurs between the vehicles, or no overtaking maneuver could be carried out by the end of the race track, the scenario ends unsuccessfully.

C. Blocking Vehicle

A kinematic bicycle model is used to specify the blocking vehicle kinematics. Omitting the time argument t for brevity and noting the derivative with respect to time as $\frac{d\Box}{dt} = \dot{\Box}$, it follows:

$$\begin{aligned} \dot{s}_b &= v_b \cdot \cos(\chi_b) \cdot \frac{1}{1 - n_b \cdot \kappa_r(s_b)} \\ \dot{n}_b &= v_b \cdot \sin(\chi_b) \\ \dot{\chi}_b &= \frac{v_b}{l_r} \cdot \sin(\beta_b) - v_b \cdot \cos(\chi_b) \cdot \frac{\kappa_r(s_b)}{1 - n_b \cdot \kappa_r(s_b)} \\ \dot{v}_b &= a_b \\ \dot{\delta}_b &= \omega_b \end{aligned} \quad (1)$$

with the body slip angle $\beta_b = \arctan\left(\frac{l_r}{l_r + l_f} \cdot \tan(\delta_b)\right)$. The state vector $\mathbf{x} = [s_b \ n_b \ \chi_b \ v_b \ \delta_b]^\top$ contains the position of the rear axle in curvilinear coordinates s_b and n_b , the relative orientation to the reference line χ_b , the absolute velocity v_b , and the steering angle δ_b . The input vector $\mathbf{u} = [\omega_b \ a_b]^\top$ consists of the steering rate ω_b and the longitudinal acceleration a_b . The distance from the center of gravity to the rear and front axle is denoted as l_r and l_f respectively. We further constrain the steering angle $|\delta_b(t)| \leq \delta_{b,max}$ and the steering rate $|\omega_b(t)| \leq \omega_{b,max}$.

For the longitudinal motion, we select $a_b(t) = 0 \text{ m/s}^2$, meaning that a constant speed is maintained. For the lateral motion, we specify the steering rate $\omega_b(t)$ based on a PD controller with parameters k_p and k_d :

$$\begin{aligned} \omega_b(t) &= k_p \cdot e(t) + k_d \cdot \dot{e}(t) \\ e(t) &= \chi_d(t) - \chi_b(t) \end{aligned} \quad (2)$$

that minimizes the error $e(t)$ between the actual vehicle orientation $\chi_b(t)$ and a desired orientation $\chi_d(t)$. The desired orientation $\chi_d(t)$ is calculated using (3) based on a desired lateral offset $\Delta \tilde{n}(t)$ and a lookahead distance parameter s_d .

In addition to the lateral distance $n_o(t) - n_b(t)$ between the overtaking and blocking vehicle, $\Delta\tilde{n}(t)$ also considers the lateral velocity, incorporating the parameter k_n .

$$\begin{aligned}\chi_d(t) &= \arctan(\Delta\tilde{n}(t) \cdot s_d^{-1}) \\ \Delta\tilde{n}(t) &= n_o(t) - n_b(t) + k_n \cdot (\dot{n}_o(t) - \dot{n}_b(t))\end{aligned}\quad (3)$$

In particular, the lookahead distance parameter s_d in the control law has a decisive influence on the aggressiveness of the blocking vehicle. The lower s_d is selected, the greater the magnitude of ω_b and the higher the aggressiveness. The step responses for different values of s_d are shown in Fig. 2.

IV. METHODOLOGY

The conventional sampling-based approach for trajectory planning of the overtaking vehicle is described in Section IV-A. Our proposed RL-based approach with the SL follows in Section IV-B and IV-C.

A. Conventional Trajectory Planning Approach

The conventional trajectory planning method is a sampling-based approach, as applied in [4], [5], [7]. A set of trajectory candidates is generated, the individual trajectories are checked for feasibility, and then the optimal valid trajectory with respect to a cost function is selected. The trajectory candidates are generated by constructing a set of longitudinal $\mathcal{T}_{\text{long}}$ and lateral curves \mathcal{T}_{lat} in curvilinear coordinates and combining each element of the two sets $\mathcal{T}_{\text{long}} \times \mathcal{T}_{\text{lat}}$. The sets are constructed by sampling end states and then connecting the vehicle state $[s_o, \dot{s}_o, \ddot{s}_o, n_o, \dot{n}_o, \ddot{n}_o]$ to them using jerk-minimal curves with a fixed temporal horizon T .

For the lateral curves $n_i(t)$, we vary the end state $\mathcal{N}_e = [n_{e,i}, \dot{n}_e, \ddot{n}_e]$ by sampling N_n equidistantly distributed positions within the track bounds $n_{e,i} \in [n_r + d_w/2, n_l - d_w/2]$, considering the vehicle width d_w . Further, the end velocity \dot{n}_e and acceleration \ddot{n}_e are set to 0 to escape the curse of dimensionality. Quintic polynomials, which are proven to be jerk-minimal [6], are used to connect the vehicle state to the sampled end states \mathcal{N}_e . Similarly, for the longitudinal curves $s_j(t)$, we vary the end state $\mathcal{S}_e = [\dot{s}_{e,j}, \ddot{s}_{e,j}]$ by sampling N_s equidistantly distributed velocities in the interval $\dot{s}_{e,j} \in [0, v_{\text{max}}]$. Again, $\ddot{s}_{e,j} = 0$ is chosen. Since the end position is not specified, the end state lies on a manifold, for which quartic polynomials are jerk-minimal [6].

Each combination of lateral and longitudinal curve $(n_i(t), s_j(t))$ is transformed into Cartesian coordinates, and the resulting trajectory is checked for feasibility. For this, we use the same three feasibility checks as in [7]. First, it is checked whether the trajectory leads to a collision with the track boundaries. Secondly, as a kinematic constraint, it is checked whether the vehicle's minimal turning radius r_{min} is not violated. Finally, as a dynamic constraint, it is checked whether the combined lateral and longitudinal acceleration lies within gg-diagrams calculated offline. In contrast to [7], in which the three-dimensional geometry of the race track impacts the gg-diagrams, here only a dependency on the velocity $v_o(t)$ is present due to the two-dimensional flat track.

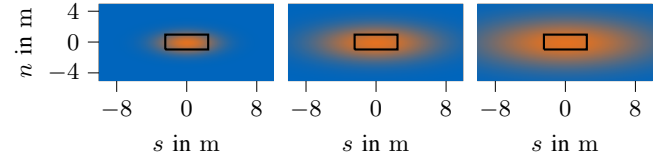


Fig. 3. Elliptical prediction cost shape for different parameterizations. The costs range from $d_{\text{pr}} = 0$ (blue) to $d_{\text{pr}} = 1$ (orange). The actual vehicle geometry is depicted in black. From left to right: small ellipse ($p_s = 0.08, p_n = 0.5$), medium ellipse ($p_s = 0.02, p_n = 0.18$), and large ellipse ($p_s = 0.01, p_n = 0.1$).

For the design of the cost function, we follow [7] and calculate the scalar cost C of a valid trajectory as

$$C = \int_0^T w_n \cdot n_o^2(t) + w_v \cdot (v_{\text{max}} - v_o(t))^2 + w_{\text{pr}} \cdot d_{\text{pr}}(t) \, dt \quad (4)$$

with the weighting parameters w_n , w_v , and w_{pr} . The first term penalizes lateral deviations from the reference line, and the second term the deviations from the maximum vehicle velocity v_{max} . The last term penalizes trajectories that are close to the prediction $(s_{b,\text{pr}}(t), n_{b,\text{pr}}(t))$ of the blocking vehicle, aiming to avoid collisions. Using the formulation

$$d_{\text{pr}}(t) = e^{-p_s[s_{b,\text{pr}}(t) - s_o(t)]^2 - p_n[n_{b,\text{pr}}(t) - n_o(t)]^2}, \quad (5)$$

an elliptical cost shape is spanned around the predicted position for each time step. The length and width can be adjusted by the parameters p_s and p_n , as shown in Fig. 3.

According to (5), the prediction significantly influences the decision on the optimal trajectory. Since the acceleration a_b of the blocking vehicle is set to 0 as described in Section III, a constant velocity model is used for the longitudinal motion prediction. For lateral movement, however, a reliable prediction is not possible, as the opponent's behavior depends on the decision of the overtaking vehicle. As these are commonly used prediction approaches, we investigate both the assumption of a constant heading (CH) and constant lateral position (CLP), with clipping of $n_{b,\text{pr}}(t)$, preventing the track boundaries from being surpassed.

B. RL-based Trajectory Planning Approach

The RL-based planning approach uses the same jerk-optimal trajectory generation as the conventional approach in Section IV-A. However, instead of generating a set of trajectories by sampling end states, the end state is explicitly selected by the RL agent, similar to [18]. This generates only a single trajectory, avoiding the need to define a cost function and the associated prediction of the blocking vehicle. A feasibility check of the planned trajectory is carried out using the same checks as the conventional approach. The corresponding MDP formulation and the utilized training procedure are presented below.

1) *State Space*: The state space of the MDP contains the vehicle state of the overtaking vehicle in curvilinear coordinates $[s_o, \dot{s}_o, \ddot{s}_o, n_o, \dot{n}_o, \ddot{n}_o]$ and its relative orientation χ_o to the reference line. It additionally includes the relative values to the blocking vehicle

$[s_o - s_b, \dot{s}_o - \dot{s}_b, n_o - n_b, \dot{n}_o - \dot{n}_b, \chi_o - \chi_b]$. All variables are normalized to lie between -1 and 1 by dividing them by the maximum possible value to accelerate the training process.

2) *Action Space*: The action space represents the end state of the trajectory in curvilinear coordinates. Although it would be conceivable to consider each end condition, we omit \ddot{s}_e in the action space and choose $\ddot{s}_e = 0$ instead. Otherwise, negative end accelerations would be selected, which allow higher accelerations at the beginning of the trajectory but do not correspond to a desired realistic trajectory. In addition, the end time T is also not included to ensure a constant planning horizon. The four-dimensional action space is thus chosen as $[n_e, \dot{n}_e, \ddot{n}_e, \dot{s}_e]$ and normalized like the state space. Note that in the conventional approach, $\dot{n}_e = \ddot{n}_e = 0$ is set for reasons of computational effort. Thus, a larger variety of trajectories can be generated with the RL-based approach.

3) *Reward Function*: The agent receives in each time step t a total scalar reward r_t , which has been designed empirically. It comprises sparse terminal rewards received at the end of an episode and a dense reward r_d during an episode that guides the agent toward the desired behavior:

$$r_t = \begin{cases} -1, & \text{if episode ends unsuccessful} \\ 10, & \text{if episode ends successful} \\ r_d, & \text{otherwise.} \end{cases} \quad (6)$$

The dense reward r_d is intended to guide the agent to successful overtakes and consists of the following two terms:

$$r_d = \frac{1}{2} (|\Delta n| - k_{\text{scl}} d_w) \cdot \mathbb{1}(s_o \in [s_b - d_l, s_b + d_l]) + (\Delta \dot{s} - \Delta \dot{s}_{\text{max}}) \cdot \mathbb{1}(\Delta \dot{s} > \Delta \dot{s}_{\text{max}}). \quad (7)$$

In this formulation, we use an indicator that specifies whether a specific condition is fulfilled:

$$\mathbb{1}(\cdot) = \begin{cases} 1, & \text{if } (\cdot) \text{ is True} \\ 0, & \text{if } (\cdot) \text{ is False.} \end{cases} \quad (8)$$

The first term in (7) rewards large lateral distances $|\Delta n| = |n_o - n_b|$ between the overtaking and blocking vehicle and is only active if the two vehicles of length d_l overlap in the longitudinal direction. Negative rewards result from distances that also lead to a lateral overlap. The vehicle width d_w is scaled with the scaling factor $k_{\text{scl}} \in [0, 1]$, which is utilized in the training procedure in Section IV-B.5. The second term rewards high longitudinal relative velocities $\Delta \dot{s} = \dot{s}_o - \dot{s}_b$ and is only active if the current relative velocity exceeds the maximum value $\Delta \dot{s}_{\text{max}}$ up to this time step.

4) *Training Algorithm and Network Architecture*: For training, we utilize the widely used PPO algorithm described in Section II consisting of an actor (policy) and a critic (value function). For both, we use fully connected neural networks as function approximators. The policy network maps from the state space (input layer dimension 12) to the action space (output layer dimension 4). The value function network also maps from the state space (input layer dimension 12) to the value of the state (output layer dimension 1). Both networks

have two hidden layers and 256 neurons per layer using the TanH activation function.

5) *Training Procedure*: We use a multi-stage curriculum learning procedure for faster and improved training in which the task's difficulty increases with each stage. In the first stage, we train the agent to generate feasible trajectories without accounting for the blocking vehicle. Accordingly, no collision checks are performed, and the term for lateral distances in the reward function (7) is omitted.

In the subsequent stages, the blocking vehicle is considered, and thus, a strategy is trained to perform successful overtaking maneuvers despite the interactive blocking behavior. In these stages, the vehicle width and length are scaled by a factor $k_{\text{scl}} \in \{0.2, 0.4, \dots, 1.0\}$ within the collision checks. With each stage, the scaling factor and, thus, the difficulty level is gradually increased until the actual vehicle geometry is used in the final sixth stage. The scaling factor k_{scl} is correspondingly incorporated into the lateral distance term in the reward function as shown in (7).

C. Safety Layer

A fundamental problem with RL-based approaches is that the feasibility of the selected trajectory is not guaranteed. Especially in scenarios not included in the training, the probability of infeasibility increases. Instead of terminating the scenario unsuccessfully in such a case as in [18], we introduce an SL intended to increase robustness and, thus, the success rate.

For this, we generate the same set of trajectories used in Section IV-A for the conventional approach when the trajectory $(s_{\text{RL}}(t), n_{\text{RL}}(t))$ selected by the RL-based approach is infeasible. All trajectories within the set are checked for feasibility so that only valid trajectories remain. In contrast to the conventional approach, cost function (4) is not used here to select the optimal trajectory. Instead, the trajectory most similar to the infeasible one chosen by the RL agent is selected. This is done using the cost function

$$C_{\text{SL}} = \int_0^T (s_{\text{RL}}(t) - s_o(t))^2 + (n_{\text{RL}}(t) - n_o(t))^2 dt. \quad (9)$$

V. RESULTS

We evaluate the conventional and the RL-based planning approach from Section IV. We start in Section V-A with computational details and explain the evaluation method used in Section V-B. The actual evaluation results for the two approaches follow in Sections V-C and V-D. Finally, the influence of the SL is examined in Section V-E.

A. Computational Details

We use gymnasium² for the implementation of the environment and the PPO implementation from Stable-Baselines3 [25]. The generated trajectories are discretized into N equidistantly distributed points in time, and the cost functions (4) and (9) are approximated according to the rectangle rule.

²<https://gymnasium.farama.org>

TABLE I
EXPERIMENT PARAMETERS

Parameter	Value	Parameter	Value
T	2.5 s	l_r	1.72 m
N_s	40	l_f	1.25 m
N_n	20	v_{\max}	85 m/s
N	51	r_{\min}	1 m
Δt	0.1 s	$\delta_{b,\max}$	0.43 rad
d_w	1.93 m	$\omega_{b,\max}$	0.39 rad/s
d_l	4.9 m		

TABLE II
EVALUATION AND TRAINING PARAMETERS

Parameter	Evaluation	Training #1	Training #2
$s_{b,\text{init}}$	$\{20, 22, \dots, 100\}$ m	$[20, 100]$ m	$[20, 100]$ m
$n_{b,\text{init}}$	$\{-6, -4, \dots, 6\}$ m	$[-6, 6]$ m	$[-6, 6]$ m
v_{init}	50 m/s	50 m/s	50 m/s
s_d	$\{40, 60, \dots, 140\}$	80	$\{40, 80, 120\}$
k_p	0.05	0.05	0.05
k_d	0.6	0.6	0.6
k_n	1.0	1.0	1.0

For the forward propagation of the blocking vehicle, the system (1) is discretized with a step size of Δt using the forward Euler method. The overtaking vehicle is propagated forward using the same time step Δt with the assumption of perfect tracking of the planned trajectory. All experiment parameters used are listed in Table I.

B. Evaluation Method

We evaluate both approaches in the blocking scenario introduced in Section III. To evaluate the generalization to different situations, we vary the initialization and the aggressiveness of the blocking vehicle. The second column in Table II shows the variation of the corresponding parameters. As stated, the initial position of the blocking vehicle ($s_{b,\text{init}}, n_{b,\text{init}}$) is varied for all six blocking behaviors shown in Fig. 2, resulting in 1722 configurations. In the following sections, we specify the success rate for each blocking behavior, i.e., for each value of s_d . This success rate, therefore, indicates the percentage of different initializations for which a successful overtaking maneuver could be executed.

C. Conventional Approach

The performance of the conventional approach depends significantly on the prediction method used and the selection of the parameters within the cost function in (4) and (5). Since a complete factorial search for the optimal cost function weight set is not possible due to the number of degrees of freedom, we evaluate six variants of the conventional approach listed in Table III. Here, the three differently sized ellipses from Fig. 3 are used, specifying the parameters p_s and p_n . Since only the relative ratio of the three remaining cost weighting parameters is relevant, we choose w_{pr} fixed for all variants. Finally, w_n and w_v are determined by a full factorial search in the value range of $[0, 1]$ with a step size of 0.04. The two options for a given ellipse shape result from a

TABLE III
COST PARAMETERS FOR CONVENTIONAL APPROACH

Parameter	Small Ellipse		Medium Ellipse		Large Ellipse	
	CH	CLP	CH	CLP	CH	CLP
p_s	0.08	0.08	0.02	0.02	0.01	0.01
p_n	0.5	0.5	0.18	0.18	0.1	0.1
w_{pr}	5000	5000	5000	5000	5000	5000
w_n	0.08	0.0	0.0	0.72	0.36	0.8
w_v	0.28	0.04	0.08	1.0	0.24	0.28

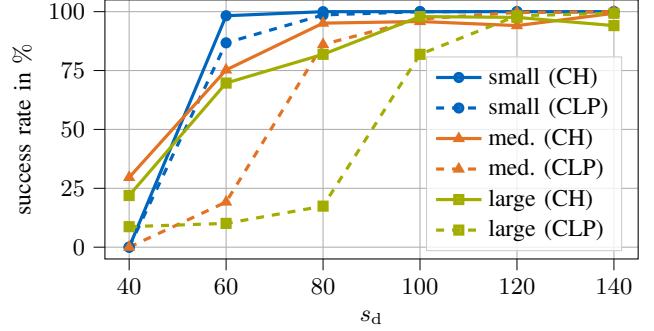


Fig. 4. Evaluation of the conventional approach with the parameterizations listed in Table III for different blocking behaviors specified by s_d . The terms small, medium (med.), and large correspond to the different ellipse sizes.

prediction based on constant heading (CH) or constant lateral position (CLP).

Fig. 4 shows the success rates of the respective variants for the different blocking behaviors. Smaller values of s_d correspond to more aggressive blocking behavior and, thus, an increased interaction. Due to the associated higher discrepancy between actual blocking behavior and prediction, the success rate generally decreases with smaller values of s_d . In addition, the CH prediction is more suitable than the CLP prediction for almost all blocking behaviors. The highest success rates of nearly 100 % for most behaviors result for the small ellipse with CH prediction. Since this cost parameterization causes low prediction costs for a large area of the race track, most overtaking maneuvers are initiated immediately, and conservative behavior is avoided. For $s_d = 40$, however, no successful overtaking maneuver can be executed since the blocking vehicle reacts at a rate that makes collision avoidance impossible with this strategy. Instead of immediately initiating an overtaking maneuver, the blocking vehicle would have to be pulled to one side of the race track to allow for an overtake on the other side with more space. However, this targeted exploitation of the interaction is not possible with the conventional approach.

D. RL-based Approach

During training, we use only a subset of the values used in the evaluation for the parameter s_d to investigate the generalization behavior of the RL-based approach to different aggressiveness levels of blocking. As listed in the third and fourth columns of Table II, we specifically distinguish two RL agents that differ in the values of s_d used during the

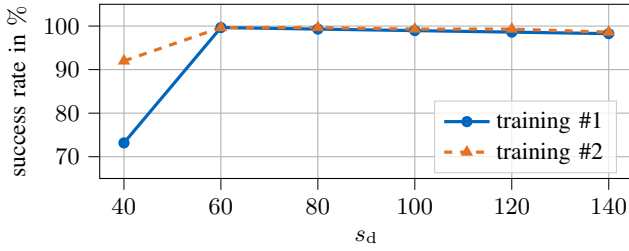


Fig. 5. Evaluation of the RL-based approach with the training parameterizations listed in Table II for different blocking behaviors specified by s_d .

training process. While only one value for s_d and thus only one blocking behavior is considered in training #1, three of the six different blocking behaviors are included in training #2. The starting position of the blocking vehicle ($s_{b,init}, n_{b,init}$), in contrast, is randomly sampled at the intervals specified in the table. The interval limits are selected as the extreme values examined in the evaluation, meaning there is no discrepancy between training and evaluation.

Fig. 5 shows the success rates for the two RL agents after training. The trajectories generated by both agents are always feasible in the examined scenarios, meaning an unsuccessful episode only occurs due to a collision. While there are only slight differences for most s_d values, more significant differences occur at $s_d = 40$, i.e., at the highest interaction level. While the success rate for agent #2 remains high with values over 90 %, it is significantly lower for agent #1, where only one value of s_d is used in the training. This demonstrates the importance of various opponent behaviors during training. For the remaining less aggressive blocking behaviors not included in the training, successful generalization is achieved with success rates close to 100 %.

Compared to the conventional approach, the success rates are higher, especially for smaller values of s_d . While the conventional approach reaches a maximum success rate of 30 % for $s_d = 40$, the RL-based approach achieves up to 92 %. This is realized by exploiting the interaction between the two vehicles, as shown in Fig. 6. The overtaking vehicle initially swerves to one side of the track, causing the blocking vehicle to move accordingly laterally. The space freed up on the other side is then exploited for a successful overtaking maneuver. In contrast, such a maneuver is not possible with the conventional approach, demonstrating the drawback of a sequential architecture consisting of prediction and planning. Furthermore, the RL-based approach has a mean computing time per planning cycle of 1.5 ms, which is 17 times shorter than the conventional approach requiring 26 ms.

E. Safety Layer

The RL agent learns to generate feasible trajectories during training. However, if a scenario deviates more strongly from the scenarios contained in the training, previously unseen states occur, which can lead to infeasibility. To prevent the episode from ending unsuccessfully in such a case, the SL presented in Section IV-C generates a valid trajectory close to the infeasible one.

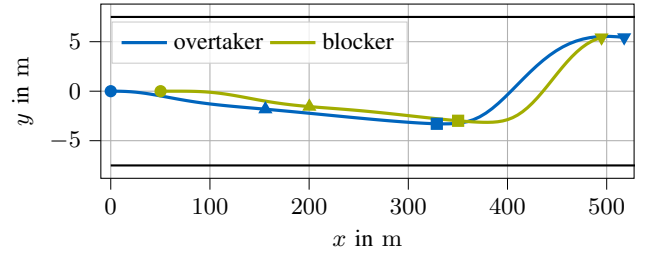


Fig. 6. Overtake using the RL-based approach with training parameterization #2 against a blocking opponent with $s_d = 40$, $s_{b,init} = 50$ m and $n_{b,init} = 0$ m. The track bounds are indicated in black, and markers of the same shape represent the same point in time.

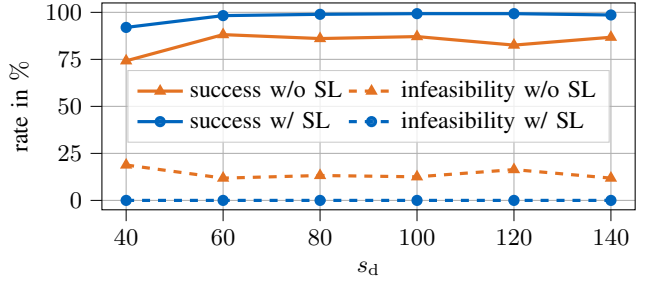


Fig. 7. Evaluation of the RL-based approach without (w/o) and with (w/) the use of the SL for different blocking behaviors specified by s_d . The training parameterization #2 listed in Table II is used with an additive gaussian noise for the opponent velocity estimation of mean $\mu = 0$ m/s and standard deviation $\sigma = 0.7$ m/s.

To investigate the effect of the SL, we rerun the evaluation for the RL-based approach but include additive Gaussian noise to the estimation of the opponent velocity \dot{s}_b , which corresponds to sensor noise in a real-world application. The noise causes states not included during training, resulting in infeasible trajectories. Fig. 7 shows the corresponding success and infeasibility rates both with and without using the SL. Here, the infeasibility rate indicates the percentage of episodes aborted due to an infeasible trajectory. Without the SL, an infeasibility rate of around 15 % results and a correspondingly low success rate. However, the infeasibility issues are entirely counteracted by the SL, achieving success rates close to the evaluation without the additional noise. The remaining unsuccessful episodes result from collisions with the opposing vehicle. However, these cases cannot be handled like infeasibility in the SL, as a collision check of a trajectory requires a prediction of the opposing vehicle, which is avoided in the RL-based approach.

VI. CONCLUSION AND OUTLOOK

This paper investigates an existing conventional sampling-based and a novel RL-based trajectory planning approach for autonomous racing in an interactive blocking scenario. The conventional approach, which relies on the prediction of the opposing vehicle, achieves high success rates for less aggressive blocking behaviors, as the prediction reflects the opposing behavior well. However, with more aggressive blocking behavior and thus a stronger interaction, the prediction loses validity, and the success rate decreases significantly. In

contrast, the RL-based approach proposed here explicitly exploits the interactive blocking behavior, allowing planning of maneuvers that are not realizable with the conventional approach. This results in high success rates even for the most aggressive blocking behavior. Here, different training configurations demonstrate the importance of various opponent behaviors for generalization. We further propose an SL that generates a sub-optimal but valid trajectory in the event of an infeasible trajectory generated by the RL agent. In the examined scenario, the SL entirely counteracts infeasibility issues and increases the success rates.

In this article, we focus on a simple scenario to demonstrate and motivate the basic principle. However, a fundamental problem with RL-based approaches is the lack of generalization to scenarios not included in training. If the RL agent used here is evaluated against an opposing vehicle that behaves differently from the blocking behavior described in this article, the success rate may decrease. Future research could, therefore, involve a generalization to more complex scenarios and race tracks. More than one opposing vehicle with respective complex behaviors could be included to force more demanding and realistic maneuvers. This would require dealing with a dynamically changing state space size or, alternatively, a fundamental change of the state space, e.g., using fixed-size 2D LiDAR sensor data. In addition, instead of a flat straight track, complex circuits and their 3D effects could be investigated, requiring an extension of the state space by track information. Furthermore, multi-agent RL, i.e., the simultaneous training of multiple agents in a single environment, is a possible extension. This avoids assumptions about the behavior of opposing vehicles, which are currently necessary. Finally, advanced network architectures such as recurrent or graph neural networks can be considered to better represent the complex interactions between agents.

REFERENCES

- [1] J. Betz, H. Zheng, A. Liniger, U. Rosolia, P. Karle, M. Behl, V. Krovi, and R. Mangharam, "Autonomous vehicles on the edge: A survey on autonomous vehicle racing," *IEEE Open Journal of Intelligent Transportation Systems*, vol. 3, pp. 458–488, 2022.
- [2] B. R. Kiran, I. Sobh, V. Talpaert, P. Mannion, A. A. A. Sallab, S. Yogamani, and P. Perez, "Deep reinforcement learning for autonomous driving: A survey," *IEEE Transactions on Intelligent Transportation Systems*, vol. 23, no. 6, pp. 4909–4926, 2022.
- [3] J. Betz, T. Betz, F. Fent, M. Geisslinger, A. Heilmeyer, L. Hermansdorfer, T. Herrmann, S. Huch, P. Karle, M. Lienkamp, B. Lohmann, F. Nobis, L. Ögretmen, M. Rowold, F. Sauerbeck, T. Stahl, R. Trauth, F. Werner, and A. Wischnewski, "Tum autonomous motorsport: An autonomous racing software for the indy autonomous challenge," *Journal of Field Robotics*, vol. 40, no. 4, pp. 783–809, 2023.
- [4] C. Jung, A. Finazzi, H. Seong, D. Lee, S. Lee, B. Kim, G. Gang, S. Han, and D. H. Shim, "An autonomous system for head-to-head race: Design, implementation and analysis; team kaist at the indy autonomous challenge." [Online]. Available: <http://arxiv.org/pdf/2303.09463v1>
- [5] A. Raji, D. Caporale, F. Gatti, A. Giove, M. Verucchi, D. Malatesta, N. Musiu, A. Toschi, S. Popitanu, F. Bagni, M. Bosi, A. Liniger, M. Bertogna, D. Morra, F. Amerotti, L. Bartoli, F. Martello, and R. Porta, "er.autopilot 1.0: The full autonomous stack for oval racing at high speeds," *Field Robotics*, vol. 4, no. 1, pp. 99–137, 2024.
- [6] M. Werling, J. Ziegler, S. Kammel, and S. Thrun, "Optimal trajectory generation for dynamic street scenarios in a frenet frame," in *2010 IEEE International Conference on Robotics and Automation*. IEEE, 2010, pp. 987–993.
- [7] L. Ögretmen, M. Rowold, A. Langmann, and B. Lohmann, "Sampling-based motion planning with online racing line generation for autonomous driving on three-dimensional race tracks," in *2024 IEEE Intelligent Vehicles Symposium (IV)*. IEEE, 2024, pp. 811–818.
- [8] L. Ögretmen, M. Rowold, M. Ochsenius, and B. Lohmann, "Smooth trajectory planning at the handling limits for oval racing," *Actuators*, vol. 11, no. 11, p. 318, 2022.
- [9] S. Aradi, "Survey of deep reinforcement learning for motion planning of autonomous vehicles," *IEEE Transactions on Intelligent Transportation Systems*, vol. 23, no. 2, pp. 740–759, 2022.
- [10] M. Jaritz, R. de Charette, M. Toromanoff, E. Perot, and F. Nashashibi, "End-to-end race driving with deep reinforcement learning," in *2018 IEEE International Conference on Robotics and Automation (ICRA)*. IEEE, 2018, pp. 2070–2075.
- [11] K. Guckiran and B. Bolat, "Autonomous car racing in simulation environment using deep reinforcement learning," in *2019 Innovations in Intelligent Systems and Applications Conference (ASYU)*. IEEE, 2019, pp. 1–6.
- [12] F. Fuchs, Y. Song, E. Kaufmann, D. Scaramuzza, and P. Durr, "Superhuman performance in gran turismo sport using deep reinforcement learning," *IEEE Robotics and Automation Letters*, vol. 6, no. 3, pp. 4257–4264, 2021.
- [13] B. D. Evans, H. A. Engelbrecht, and H. W. Jordaan, "High-speed autonomous racing using trajectory-aided deep reinforcement learning," *IEEE Robotics and Automation Letters*, vol. 8, no. 9, pp. 5353–5359, 2023.
- [14] D. Loiacono, A. Prete, P. L. Lanzi, and L. Cardamone, "Learning to overtake in torcs using simple reinforcement learning," in *IEEE Congress on Evolutionary Computation*. IEEE, 2010, pp. 1–8.
- [15] Y. Song, H. Lin, E. Kaufmann, P. Durr, and D. Scaramuzza, "Autonomous overtaking in gran turismo sport using curriculum reinforcement learning," in *2021 IEEE International Conference on Robotics and Automation (ICRA)*. IEEE, 2021, pp. 9403–9409.
- [16] P. R. Wurman, S. Barrett, K. Kawamoto, J. MacGlashan, K. Subramanian, T. J. Walsh, R. Capobianco, A. Devlic, F. Eckert, F. Fuchs, L. Gilpin, P. Khandelwal, V. Kompella, H. Lin, P. MacAlpine, D. Oller, T. Seno, C. Sherstan, M. D. Thomure, H. Aghabozorgi, L. Barrett, R. Douglas, D. Whitehead, P. Dürr, P. Stone, M. Spranger, and H. Kitano, "Outracing champion gran turismo drivers with deep reinforcement learning," *Nature*, vol. 602, no. 7896, pp. 223–228, 2022.
- [17] R. Trauth, A. Hobmeier, and J. Betz, "A reinforcement learning-boosted motion planning framework: Comprehensive generalization performance in autonomous driving," in *2024 IEEE Intelligent Vehicles Symposium (IV)*. IEEE, 2024, pp. 2413–2420.
- [18] B. Mirchevska, M. Werling, and J. Boedecker, "Optimizing trajectories for highway driving with offline reinforcement learning," *Frontiers in Future Transportation*, vol. 4, 2023.
- [19] A. Liniger and J. Lygeros, "A noncooperative game approach to autonomous racing," *IEEE Transactions on Control Systems Technology*, vol. 28, no. 3, pp. 884–897, 2020.
- [20] M. Wang, Z. Wang, J. Talbot, J. C. Gerdes, and M. Schwager, "Game-theoretic planning for self-driving cars in multivehicle competitive scenarios," *IEEE Transactions on Robotics*, vol. 37, no. 4, pp. 1313–1325, 2021.
- [21] R. S. Sutton and A. G. Barto, *Reinforcement Learning: An Introduction*, 2nd ed., ser. Adaptive computation and machine learning. Cambridge, Massachusetts and London, England: The MIT Press, 2018.
- [22] J. Schulman, F. Wolski, P. Dhariwal, A. Radford, and O. Klimov, "Proximal policy optimization algorithms." [Online]. Available: <http://arxiv.org/pdf/1707.06347v2>
- [23] Y. Bengio, J. Louradour, R. Collobert, and J. Weston, "Curriculum learning," in *Proceedings of the 26th Annual International Conference on Machine Learning*, A. Danyluk, L. Bottou, and M. Littman, Eds. New York, NY, USA: ACM, 2009, pp. 41–48.
- [24] S. Narvekar, B. Peng, M. Leonetti, J. Sinapov, M. E. Taylor, and P. Stone, "Curriculum learning for reinforcement learning domains: A framework and survey," *Journal of Machine Learning Research*, vol. 21, no. 181, pp. 1–50, 2020.
- [25] A. Raffin, A. Hill, A. Gleave, A. Kanervisto, M. Ernestus, and N. Dormann, "Stable-baselines3: Reliable reinforcement learning implementations," *Journal of Machine Learning Research*, vol. 22, no. 268, pp. 1–8, 2021.